

TRANSIENT AND SMALL SIGNAL STABILITY OF A TWO AREA HVAC POWER NETWORK INTERCONNECTED WITH AN HVDC LINK

L.C Azimoh, D.T Oyedokun, S. Chowdhury, S.P Chowdhury, K.A Folly

Electrical Engineering Department, University of Cape Town

Private Bag X3, Rondebosch, Cape Town 7701, South Africa

Leonard.azimoh@uct.ac.za, davoyedokun@ieee.org, spchowdhury@uct.ac.za, komla.folly@uct.ac.za

ABSTRACT

This paper presents an analysis of transient and small signal stability of a two-area multi machine power system. This is achieved by investigating the responses of generator speed, the terminal voltage, the rotor angle difference and power transmitted, after a transient perturbation of a single phase to ground fault. Furthermore, the study shows the effect of small signal disturbance of power systems when a dc link is interconnected with a weak ac link.

The small signal stabilities of three different transmission systems are investigated, using the two-area power system model. The following three cases are used for the study of small signal stability study - High Voltage Alternating Current (HVAC) Link, High Voltage Direct Current (HVDC) Link and the hybrid HVAC/HVDC link. The transient stability was investigated on the hybrid HVAC/HVDC by applying a single phase to ground fault at middle of the line L9 of HVAC line on the hybrid power network. This study shows that even when the parent networks HVAC and HVDC are stable, their interaction could affect the stability of the power network if the tie between them is weak.

KEY WORDS

HVDC, HVAC, Transient stability, small signal stability, eigenvalue

1. Introduction

The responsibility of power system operators is to supply electric power safely and economically to customers, despite the fact that the conditions necessary for safe and stable operation of power networks are sometimes at variance with economic considerations. Operators are also compelled by market forces to meet the demand of the customers in the most economic and efficient manner in order to gain a good market share. The demand of the customers cannot be met without a stable and reliable power supply. Therefore, power system stability is of paramount importance in this market. Furthermore, with the commercialization and deregulation of power and energy industry by various governments across the world, some customers in power sector of the economy gravitate to those companies that can guarantee the best power

quality. Therefore, stability and efficiency has become a watchword for setting up a successful power utility company in the industry. In Power Engineering literature, stability is defined as follows: *“Power System Stability is the ability of an electric power system, for a given initial operating condition, to regain a state of operating equilibrium after being subjected to a physical disturbance, with most system variables bounded so that practically the entire system remains intact”* [1].

Stability is essential for a reliable and dependable power supply. Power system stability has been a complex problem and has challenged system engineers since early 20th century till date. Transmission of power over a long distance imposes some strains on the network, and furthermore load characteristics and switching activities are sources of disturbance within the network that may cause stability problems. Transient stability is the ability of a power system to maintain synchronism after experiencing a transient perturbation like lost of generating unit, severe overload, etc. The system maintains synchronism after being subjected to a major disturbance. A stable power network must be able to maintain a steady-state or attain a new steady state of operation after a fault [2]. In this paper, a weak HVAC system is interconnected with an HVDC system to investigate their interaction with respect to small signal and transient disturbances and three case studies are investigated altogether. In the first case HVAC/HVDC is studied. In the second case, only the HVAC link is investigated and in the third case, only the HVDC link is investigated. A single phase to ground fault is applied on HVAC line L9 to investigate the transient stability. The complex nature of HVAC-HVDC interactions poses some difficulties in modeling of these systems and these are the main reasons for the lack of analytical background to this problem [3]. As stated above, rotor angle stability is an embodiment of both transient and small signal stability, its study has to do with the electromechanical oscillations embedded in the power network. Small signal stability is the ability of a power system to maintain synchronism under small perturbation. It is associated with lack of sufficient damping torque resulting in oscillatory instability or lack of synchronizing torque resulting in non-oscillatory or a-periodic mode [1]. Small signal

stability can be in the form of local or inter area oscillations. Recent papers have proposed solutions to the problem of inter area oscillations by using power systems stabilizers (PSS), Flexible AC transmission systems (FACTS) and HVDC Links to damp inter area oscillations [4]. Both local and inter-area oscillations are discussed in this paper

The authors of this paper addresses ways of improving power network stability and reliability with special emphasis on the transient stability and small signal stability.

2. Fundamentals of HVAC Transmission

Fundamentally, the parameters of a transmission line are the shunt conductance, the series resistance, series inductance and the shunt capacitance. These parameters are distributed within the network and so are their effects.

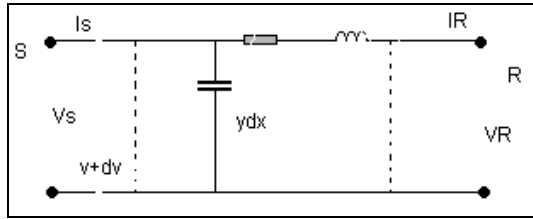


Figure 1: Equivalent circuit of transmission line

The voltage and current relationship for the sending and receiving ends are given as in equations 1 and 2.

$$V_S = V_R \frac{e^{\gamma l} + e^{-\gamma l}}{2} + Z_C I_R \frac{e^{\gamma l} - e^{-\gamma l}}{2} \quad (1)$$

$$I_S = I_R \text{Cosh}(\gamma l) + \frac{V_R}{Z_C} \text{Sinh}(\gamma l) \quad (2)$$

V_S is the sending end voltage, V_R is the receiving end voltage, Z_C is the characteristic impedance of the transmission line, γ is propagation constant and l is the length.

The power transmitted in a power network is as given in the equations 3 and 4,

$$P_S = \frac{E_S E_R}{X} \text{Sin} \delta \quad (3)$$

$$Q_S = \frac{-E_S (E_R \cos \delta - E_S \cos \theta)}{X} \quad (4)$$

where, P_S represents the active power at the sending end of the transmission network, Q_S represents the reactive power at the sending end of the transmission network, E_S and E_R represents voltages at sending and receiving ends respectively and X is the reactance of the transmission line. δ is the phase angle displacement between the sending end and receiving end voltages of the

transmission line, θ represents the electrical length or line angle. In a lossless line, when $R = 0$, maximum power is transferred when δ equals 90° .

The control of these parameters determines the power transmitted along transmission lines in power networks.

3. Fundamentals of HVDC Transmission

In HVDC transmission, the conversion of AC to DC occurs at the transmitting end (rectifier) and the inversion of DC to AC occurs at the receiving end (inverter). Converters consist of high voltage bridges and tap changing transformers while valve bridges consist of high voltage valves connected in 6-pulse or 12-pulse arrangement. One of the advantages of this technology is the fault-blocking characteristics of the system which enables it to serve as an automatic firewall for blackout prevention in case of cascading events, which is impossible with flexible alternating current transmission system (FACTS) [5].

Power flow equation of HVDC line is given as follows:

$$P_d = V_d \cdot I_d \quad (5)$$

$$Q_R = P_d \cdot \tan \gamma \quad (6)$$

$$I_d = \frac{V_{dor} \text{Cos} \alpha - V_{doi} \text{Cos} \gamma}{R_{cr} + R_L - R_{ci}} \quad (7)$$

and

$$V_d = V_{do} \cos \gamma - \frac{3}{\pi} X_c I_d B \quad (8)$$

V_d , I_d are the direct voltage and current per pole respectively, α is the firing angle of the rectifier, B stands for the number of bridges in series and γ is the extinction angle. V_{dor} , V_{doi} are the voltages at rectifier and inverter respectively. Z_C and X_C are the characteristic impedance and commutating reactance respectively. R_{cr} , R_{ci} and R_L are the resistances at rectifier, inverter and the DC line respectively. P_d Represents the active power transmitted, while Q_R represents the reactive power at the AC bus.

In HVDC power transmission, the time taken for the current to move from one phase to another is known as overlap time or commutation time because the line inductance of AC source phase currents do not change instantly. The angle associated with this is known as overlap angle or commutation angle (μ). In normal operation μ values are less than 60° . Typical full load values are in the range of 15° to 25° and normal operation is $15^\circ - 45^\circ$ therefore, the range is $15^\circ < \mu < 60^\circ$ [6].

4. Rotor Angle Stability

The ability of interconnected synchronous machines to maintain synchronism after being subjected to a fault is referred to as rotor angle stability [1]. The equilibrium of electromagnetic and mechanical torque of the participating synchronous machines determines the stability. Furthermore, for stable operation, all the currents and voltages within the power system must operate at the same frequency and the rotor speed of each participating machine must synchronize to this frequency. In steady state of operation the input mechanical torque and output electrical torque of each machine must be in equilibrium, with the speed remaining constant.

Therefore, during perturbation this equilibrium is upset resulting in either acceleration or retardation of the rotors of the machines. This disturbance causes one or several machines to run faster than the rest, depending on the point of application of fault. At this point more loads is transferred to the faster machine which slows steadily and consequently allows the slower machine's speed to meet up and synchronize with the faster one, thereby reaching a steady state of operation.

The speed difference brings about angular separation and an increase in angular separation leads to decrease in power transfer. When stretched further the system goes into instability. Change in electrical torque of a synchronous machine following a disturbance can be resolved into two components as given in equation 9. [7]

$$\Delta T_e = T_s \Delta \delta + T_D \Delta \omega \quad (9)$$

Where, ΔT_e is the change in electrical torque. ($T_s \Delta \delta$) is the component of the torque change in phase with rotor angle perturbation, known as the synchronizing torque. ($T_D \Delta \omega$) is the component of torque in phase with the speed deviation, known as damping torque coefficient. Lack of these, in power system results in instability through a-periodic drift and damping torque oscillatory instability respectively.

Generally, the machine rotor movement is governed by Newton's second law of motion [8] as given below in equation 10.

$$J \alpha_m(t) = T_m(t) - T_e(t) = T_a(t) \quad (10)$$

Where,

J = total moment of inertia of a rotating mass, kg

T_a = net accelerating torque, Nm

T_e = electrical torque, Nm

T_m = mechanical torque, Nm

α_m = rotor angle acceleration, rad/s²

Two types of rotor angle stability that are considered in the following section are transient and small signal stability.

4.1 Transient stability

Transient stability depends largely on the initial operating conditions and the severity of the transient disturbance. This could be due to loss of generating units or loss of

major loads. This instability occurs when rotor speed increases steadily until synchronism is lost within the first second, this situation is known as first swing instability and it is caused by lack of sufficient synchronizing torque. However, in large power systems, various oscillations that advance the rotor angle beyond the first swing can cause it also.

4.2 Small Signal Stability

The prevailing situation in power system suggests that small signal stability problems emanate largely from insufficient damping of oscillations. Small signal stability modes have been classified as follows [1]:

Local mode: This occurs when one or more generators in a station swings against the rest of the generators within a location. Their effects thus are localized.

Inter-area mode: This happens when a group of generators in the network in one location swings against the rest of the generators in the network. This is peculiar to networks with weak short circuit ratio (SCR).

Other modes are control modes due to control devices within the network i.e. HVDC controls, Static Var Compensator (SVC) and speed governors, etc. Also, torsional mode is another mode inherent in power systems, which could be attributed to turbine generator shaft system rotational systems.

5. HVAC/HVDC Hybrid Network Model

A two area power system model taken from [2] is used for the simulations as shown in Fig.2. The AC network parameter, as given in the above reference was used under a 50Hz system in this study. CIGRE parameters are also used for the converter stations for DC network. The parameters used are as follows:

(i) Generator rated values are 20KV, 900MW, 50Hz.

(ii) The total HVAC line length is set at 420km and HVDC line was set at 2000km.

(iii) The rectifier station is set at constant current control; the rated current is 2 kA whilst the inverter station is set at gamma (Constant extinction angle) control.

(iv) A single phase to ground fault is applied at 50% of the line length on the HVAC line for 3 seconds and cleared after 3.05 seconds, under a 50Hz power system.

(v) The Generator (G1) on the left area A is the slack bus and the one on the right (G3) in area B was set as a PV bus and G2 and G4 are set as PQ bus.

6. Simulation Results

In this section the results obtained from the simulations are presented as follows:

6.1 Power Flow

In Appendix Table A: 1. The load flow result indicates that the total power generated by the four generators into the network is about $(2772.83 + j300)$ MVA and the installed capacity is around 3240MW. Total power amounting to $(400 - j100)$ MVA flows from area A to area B in order to meet the load demand of $(1805.83 + j200)$ MVA of area B, which is greater than the generated power $(1417.33 + j328.02)$ in area B. The additional

reactive power requirement is compensated by the $(j350)$ MVAR from capacitor (C9) to reduce the characteristics impedance and thereby improve the power level. Generators at area one supplied $(1402 + j67.14)$ MVA to meet the demand of $(967 + j100)$ MVA of the load GL7 in area B. The excess power is transmitted by both the HVDC and HVAC to meet the demand at area B. The total power loss in the system is $(50.32 + j276.36)$ MVA.

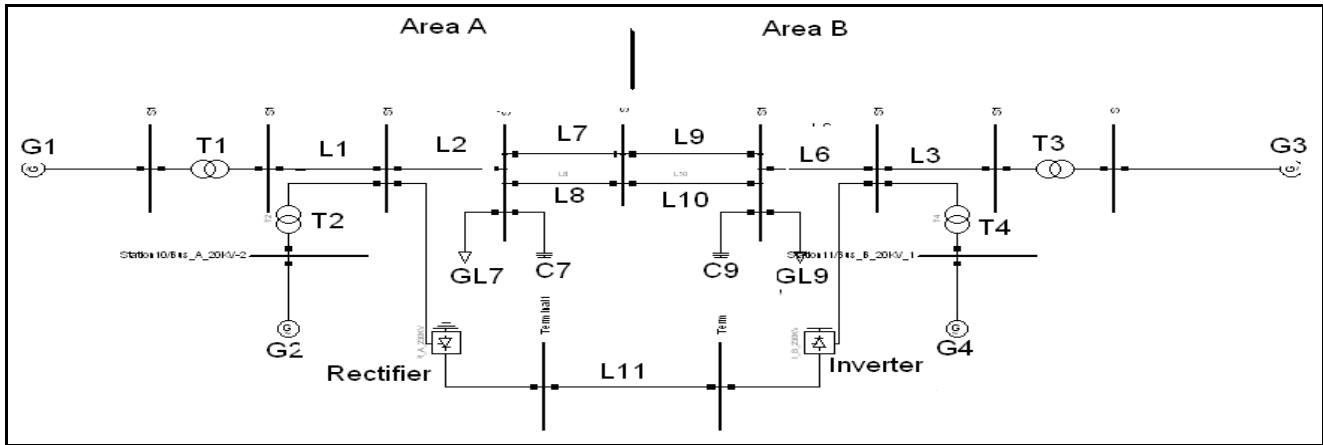


Figure 2. Two Area Network System

Figures 3-8 Shows the results of transient simulation

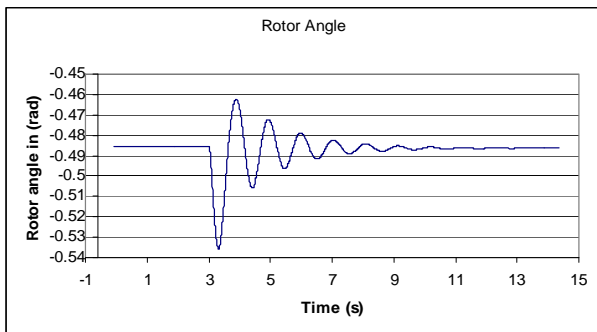


Figure 3. Generator (G3) Rotor Angle Stability

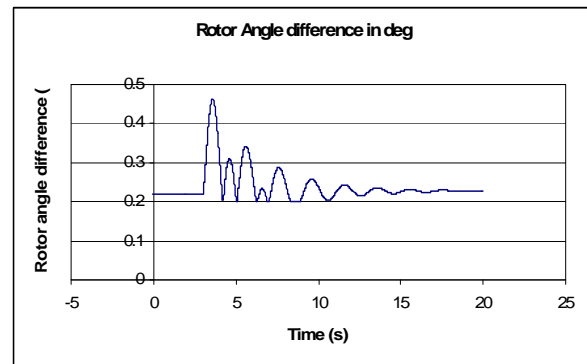


Figure 5. Rotor Angle difference (G1)

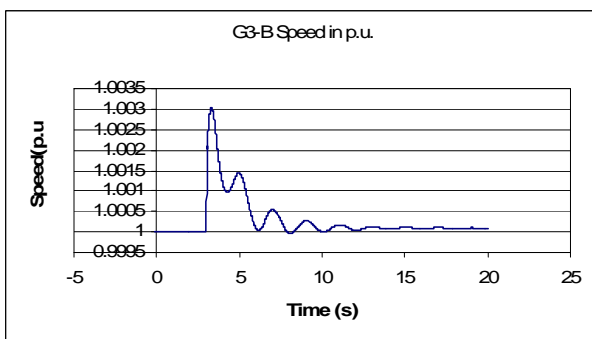


Figure 4. Generator (G3) Speed

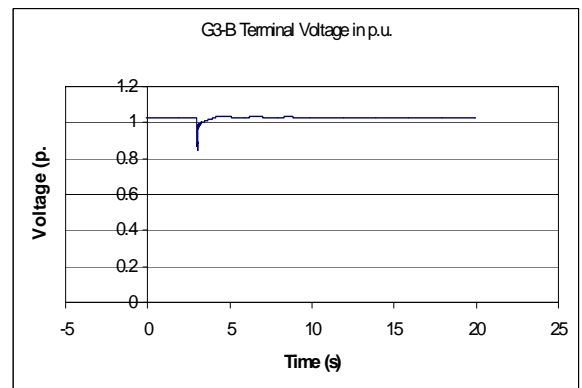


Figure 6. Terminal Voltage of Generator (G4)

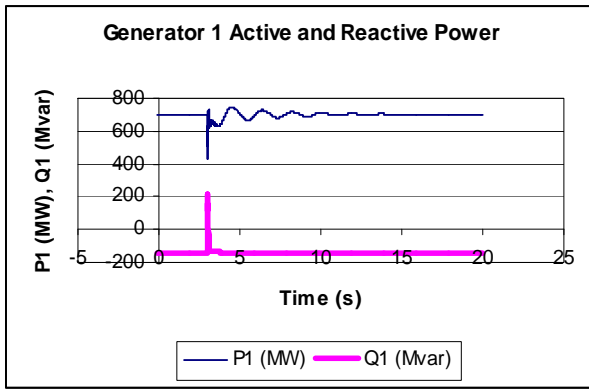


Figure 7. Active and Reactive Power of (G3)

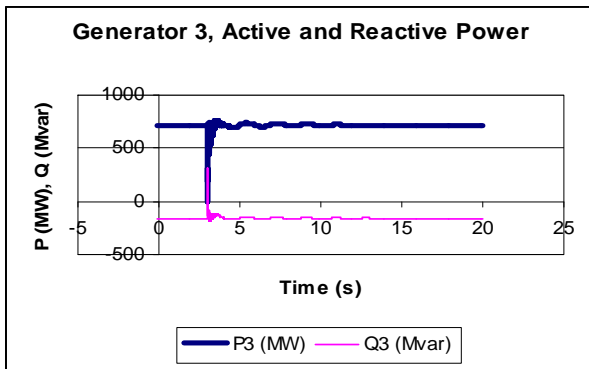


Figure 8. Active and reactive power of generator (G1)

6.2 Transient Stability Analysis

Transient stability is investigated using the hybrid link as the test case. Figures 3 to 8 above show the effects of the transient disturbance (single phase to ground fault) in line L9 with regard to rotor angle stability, generator speed, maximum rotor angle difference, terminal voltage of generator and generator active and reactive power. Figure 3 shows generator G1's rotor angle response to the perturbation. In the first swing it dipped from -0.485 rad to about -0.538 rad and then up to about -0.463 rad before stabilizing.

Figure 4 shows that the speed of the generator (G3) swing from 1.0 p.u. (pre-fault steady state operating condition) to about 1.0045 p.u. before coming to a steady state of operation after about 10 seconds following the transient disturbance. It is to be noted that G3 is investigated because it is close to the fault. Figure 5 shows that the rotor angle difference of generator G1 was at 60° before the fault, but swings to about 61.9° and then dipped to about 58.5° before coming to equilibrium at 60° after about 10 seconds post fault situation. Figure 6 shows the behavior of the terminal voltage of generator G3 following the fault. The system was operating at about 1.038 p.u. before the fault, but dipped after the fault to about 0.997 p.u. during the fault, before recovering to a stable state of operation at about 8-9 seconds after the fault.

Following the fault, active and reactive powers of generators 3 and 1 are temporally perturbed as indicated

by Figure 7 and 8. G3's active power has a downward swing from about 700 MW to about 100MW this follows some ripples before returning to a stable state after about 8 seconds after the perturbation, the reactive power followed similar pattern but in opposite direction. The first swing was upward from about -190Mvar operating state to about 300 Mvar before coming to rest. G1's first swing is downwards from about 700 MW to about 400MW before returning to steady state of operation within 8-10 seconds after the disturbance. The reactive power of G1 had an upward swing following the fault from about -100 Mvar to about 200 Mvar following the first swing and returns to a steady state after about 8 seconds following the fault.

6.3 Small Signal Stability Analysis

Theoretically the inter-area oscillation frequency ranges from 0.1 to 0.3 Hz for very low frequency and from 0.4 to 0.8 Hz for low frequency. Local mode and inter-machine mode is within the range of 0.8 to 2 Hz. Frequency of oscillation depends on the strength of the system and on the moment of inertia of the generator rotors [2]. Using Lyapunov's 1st method, when the eigenvalues of a system have negative real part, the original system is asymptotically stable. When the eigenvalues have at least a positive real part the original system is unstable and when eigenvalues have a real part equal to zero, it is not possible on the basis of first approximation to say anything in general about the stability [9].

Tables 1-3 Shows the Small Signal simulation results for the three case scenarios.

Table 1. HVAC/HVDC

Mode	Real Part	Imaginary part	Damped Frequency	Damping Ratio
1	0	0	0	0
2	-28.1826	0	0	1
3	-32.0859	0	0	1
4	-31.3876	0	0	1
5	-30.3150	0	0	1
6	-9.9288	0.0355	0.0056	0.9999
7	-9.9288	-0.0355	0.0056	0.9999
8	-1.1919	6.9331	1.1034	0.1694
9	-1.1919	-6.9331	1.1034	0.1694
10	-1.2157	6.7780	1.0788	0.1765
11	-1.2157	-6.7780	1.0788	0.1765
12	-0.3038	3.1662	0.5039	0.0955
13	-0.3038	-3.1662	0.5039	0.0955
14	-4.1803	0	0	1
15	-3.6676	0	0	1
16	-0.9929	0	0	1
17	0.0102	0	0	-1
18	-0.0414	0	0	1
19	-0.0363	0	0	1
20	-0.0363	0	0	1

Table 2. HVDC Small Signal Disturbance result

Mode	Real Part	Imaginary Part	Damped Frequency	Damping Ratio
1	0	0	0	0
2	-31.1888	0	0	1
3	-28.3979	0	0	1
4	-31.4161	0	0	1
5	-27.9120	0	0	1
6	-10.0043	0	0	1
7	-1.2483	6.8623	1.0922	0.1790
8	-1.2483	-6.8623	1.0922	0.1790
9	-9.1161	0	0	1
10	-4.0000	0	0	1
11	-1.7562	6.3687	1.0136	0.2658
12	-1.7562	-6.3687	1.0136	0.2658
13	-2.8637	0	0	1
14	-1.0680	0	0	1
15	-0.9447	0	0	1
16	-0.0514	0	0	1
17	-0.0000	0	0	1
18	-0.0244	0	0	1
19	-0.0335	0.0068	0.0011	0.9799
20	-0.0335	-0.0068	0.0011	0.9799

Table 3. HVAC Small Signal Disturbance result

Mode	Real part	Imaginary part	Damped Frequency	Damping Ratio
1	0	0	0	0
2	-31.2941	0	0	1
3	-31.3799	0	0	1
4	-28.7799	0	0	1
5	-28.1394	0	0	1
6	-9.9626	0	0	1
7	-9.8757	0	0	1
8	-1.2129	7.0157	1.1166	0.1704
9	-1.2127	-7.0157	1.1166	0.1704
10	-1.2222	6.890	1.0966	0.1747
11	-1.2222	-6.890	1.0966	0.1747
12	-0.4244	3.6371	0.5789	0.1159
13	-0.4244	-3.6371	0.5789	0.1159
14	-5.5045	0	0	1
15	-3.7751	0	0	1
16	-0.9892	0	0	1
17	-0.0015	0	0	1
18	-0.0390	0	0	1
19	-0.0333	0	0	1
20	-0.0293	0	0	1

6.3.1 HVAC/HVDC Link

Table 1 gives the modes that represent the states of the generators in the system and the Eigenvalues are represented by the real and imaginary parts. Modes 2 to 5, 14 to 16 and 18 to 20 are real eigenvalues with damping ratio of 1 and these represent stable eigenvalues which are said to be critically damped. Modes 6 and 7 are conjugate pairs with collective damping ratio of 0.9999. Similarly, modes 12 and 13 are conjugate pairs with a lower damping ratio of 0.0955. It shows that the eigenvalues are stable with decaying oscillations. These are the dominant eigenvalues in the system.

From the above analysis, it can be concluded that the HVDC/HVAC hybrid system stability is unstable under small signal disturbance, and the dominant oscillation mode in the system local area and inter-machine

oscillations. The instability is due to the dominance of negative damping ratio in the 17th mode. Despite the presence of a real positive mode and a negative damping ratio in the 17th mode, the system remains stable, because it is not a dominant mode in small signal analysis. The behavior of this mode could be attributed to load flow convergence error which needs further investigation.

6.3.2 HVDC Link

In Table 2, the HVDC result shows that modes 2 to 6, 9 to 10 and 13 to 18 are critically damped. The dominant mode of oscillation here is local mode. There are no inter area oscillations but there are traces of control mode of oscillation at the 19 and 20 modes which are well damped. To this end, the system can be said to be very stable under small signal disturbance, since the presence of the HVDC system does not allow the local mode to fade into inter-area mode of oscillation.

6.3.3 HVAC Link

From Table 3, modes 2 to 6 and 14 to 20 are real eigenvalues with damping ratio of 1. This represents the highest eigenvalues that can be achieved. Modes 8 and 9, and 10 and 11 are conjugate pairs with damping ratios 0.1704Hz, 0.1747Hz and frequencies 1.1166Hz and 1.0966Hz respectively. This represents local mode of oscillation in the system. Also, modes 12 and 13 are conjugates and represent inter-area oscillation with damped frequency of 0.5789 and damping ratio of 0.1159 which indicates that the system is poorly damped. However it represents stable eigenvalues with decaying oscillations.

From the above analysis, the HVAC system is stable. Applied fault excites both local and inter-area modes of oscillation in Area 1 of generators G1 and G2. Also, Area 2 with generators G3 and G4 have both oscillations, but the local oscillations die off before fading into inter area modes. This is justified by the fact the local mode has higher damping factor than the inter-area mode.

7. Conclusion

From the above analysis of the results, the transient stability test shows that the system is relatively stable. It returns to pre-fault condition state on the average of about 10 seconds after perturbation.

The analysis of the small signal stability shows that even though the parent networks (HVDC, HVAC) are stable, the hybrid network (HVDC/HVAC) is found to be unstable due to weak interaction between the two networks as indicated in mode 17.

For this reason it advisable to interconnect systems with high SCR, this gives a better performance for the hybrid network. Further investigation on the participation factors of the systems within the network is recommended to find out the part played by each of elements in the system. This will enable a better understanding of the problem.

This study has clearly demonstrated that when a fault occurs in transmission lines the system responds

according to the nature of fault and the strength of the system, the knowledge of this will assist network planners to design for contingencies. The major limitation of this study is that, there was no provision in DIGSILENT Power Factory software to identify participation factors of the systems. Also, due to the complex nature of HVDC and HVAC interconnections modeling of this system was difficult. In future, investigation on the system parameters will be carried out with a view of finding out the effect of its participation factor in the power network.

Acknowledgement

The authors are pleased to acknowledge the support provided by the Department of Electrical Engineering, University of Cape Town.

References

- [1] Prabha Kundur, John Paserba, Goran Anderson Anjan Bose, Claudio Canizares, Nikos Hatziar gyriou, David Hill, Alex Stankovic, Thierry Van Cutsem and Vijay Vittal: "Definition and Classification of Power System Stability", *IEEE/CIGRE Joint Task Force on Stability Terms and Definitions. IEEE Transaction on power systems, Vol. 19, No.2, May 2004.*
- [2] Prabha Kundur: "Power system stability and control" 1994 Edition.
- [3] Dragan Jovcic, Nalin Pahalawaththa, Mohamed Zavar, "small signal analysis of HVDC-HVAC interactions". *IEEE Transaction on Power Delivery, Vol, 14, No. 2, April 1999.*
- [4] R.Witzmann, "Damping of inter-area oscillations in a large interconnected power systems", *Dept. EV SE NC3, Siemens, P.O. Box 3220, D-91050 Erlangen, Germany.* [http:// www.mhhc.com](http://www.mhhc.com)
- [5]W. Breuer, D. Povh, D. Retzmann, Teltsch and X. Lei, "Role of HVDC and FACTS in future power systems review paper". *CEPSI Shanghai, 2004.*
- [6] J. C Das: "Power systems analysis", New York, Marcel Dekker, 1934, c2002.
- [7] Hadi Saadat "Power System Analysis". Schaum's Outline series in Electrical and Electronics Engineering. Copyright © 1999 by McGraw-Hill Companies
- [8] J. Duncan Glover and Sarman, "Power system analysis and design", 3rd edition, 2002 pp 608-643
- [9] Graham Rogers: "Power system oscillations", The Kluwer international series in Engineering and Computer science, series editor: M. A Pai, 2000 Edition.

Appendix

Table A.1. the table shows power flow in the system from area a to area B

		Active Power (MW)	Reactive Power (Mvar)
G1 Area A	Station 1	704.15	-498.30
T1-A		704.15	-498.30
G2-A	Station 10	700.00	235.00
T2-A		700.00	235.00
T3-B	Station 9	719.00	4.31
G3-B		719.00	4.31
G4 Area B	Station 11	700.00	202.00
T4-B		700.00	202.00
L1-A	Station 2	704.15	-521.68
T1-A		-704.15	521.68
L1-A	Station 3	-702.33	14.14
L2-A		1110.50	20.63
T2-A		-700.00	-220.53
REC-A	Station 7	291.82	185.76
GL7-A	Station 4	967.00	100.00
C7-A			-246.36
L2-A		-1106.18	32.37
L7-A		69.59	56.99
L8-A		69.59	56.99
L10-B	Station 5	69.30	53.49
L7-N		-69.30	-53.49
L8-B		-69.30	-53.49
L9-B	Station 6	69.30	53.49
L3-B	Station 7	-717.23	141.96
L6-B		1679.05	-148.90
T4-B		-700.00	-186.06
L3-B	Station 8	719.00	-11.93
T3-B		-719.00	11.93
G3-B	Station 9	719.00	4.31
T3-B		719.00	4.31
L11-B	Terminal 12	-261.82	0.00
Inverter-B		261.82	0.00
GL9-B		1805.83	200.00
C9-B	Station 6	0.00	-400
L11-B	Terminal 11	291.82	0.00
REC-A		291.82	0.00